



Enriched cell-free and cell-based native membrane derived vesicles (nMV) enabling rapid in-vitro electrophysiological analysis of the voltage-gated sodium channel 1.5

Yogesh Pandey^{a,b}, Srujan Kumar Dondapati^{a,*}, Stefan Kubick^{a,c,d,e}

^a Fraunhofer Institute for Cell Therapy and Immunology (IZI), Branch Bioanalytics and Bioprocesses (IZI-BB), Am Mühlenberg 13, 14476 Potsdam, Germany

^b Institut für Biochemie und Biologie, University of Potsdam, Karl-Liebknecht-Str. 24-25, 14476 Potsdam OT Golm, Germany

^c Technische Universität Berlin, Institute of Biotechnology, Straße des 17. Juni 135, 10623 Berlin, Germany

^d Freie Universität Berlin, Institute of Chemistry and Biochemistry, 14195 Berlin, Germany

^e Faculty of Health Science, Joint Faculty of the Brandenburg University of Technology Cottbus-Senftenberg, the Brandenburg Medical School Theodor Fontane and the University of Potsdam, Germany

ARTICLE INFO

Keywords:

Cell-free protein synthesis
Electrophysiology
Membrane proteins
Micro-transplantation
Protein expression

ABSTRACT

Here, we demonstrate the utility of native membrane derived vesicles (nMVs) as tools for expeditious electrophysiological analysis of membrane proteins. We used a cell-free (CF) and a cell-based (CB) approach for preparing protein-enriched nMVs. We utilized the Chinese Hamster Ovary (CHO) lysate-based cell-free protein synthesis (CFPS) system to enrich ER-derived microsomes in the lysate with the primary human cardiac voltage-gated sodium channel 1.5 (hNav_v1.5; SCN5A) in 3 h. Subsequently, CB-nMVs were isolated from fractions of nitrogen-cavitated CHO cells overexpressing the hNav_v1.5. In an integrative approach, nMVs were micro-transplanted into *Xenopus laevis* oocytes. CB-nMVs expressed native lidocaine-sensitive hNav_v1.5 currents within 24 h; CF-nMVs did not elicit any response. Both the CB- and CF-nMV preparations evoked single-channel activity on the planar lipid bilayer while retaining sensitivity to lidocaine application. Our findings suggest a high usability of the quick-synthesis CF-nMVs and maintenance-free CB-nMVs as ready-to-use tools for in-vitro analysis of electrogenic membrane proteins and large, voltage-gated ion channels.

1. Introduction

Conventionally, analysis of ion-channel receptors is performed by directly expressing the channels in cellular systems. In the last 50 years, these systems have markedly facilitated our understanding of macroscopic and single-channel properties of the ion-channel function [1]. However, these biological systems have a long-standing disadvantage. They require extensive culturing, maintenance, and harvesting before testing. In the last two decades, new technological advancements have enabled the study of membrane proteins in-vitro, both in their native and artificial membrane environments. These encompass plasma membrane blebs, integral membrane patches, artificial lipid-reconstituted giant plasma membrane vesicles (GPMVs), proteo-liposomes, and giant unilamellar vesicles (GUVs) [2]. The developments have further elucidated the role of proteins under controlled membrane lipid

compositions and their effects on channel integration and function.

These methods have enabled the study of electrogenic proteins like ion channels and transporters in-vitro under both physiological and artificial ionic environments. Despite the advances, most of these methods have relied on protein reconstitution into extraneous lipid environments before testing with direct use of crude plasma membranes finding only limited use [3]. Recent reports on probing sugar transporters over a solid-supported membrane and porins from bacterial outer membranes have furthered the potential of directly using cell-based membranes for electrophysiological analysis [4].

In the last decade, Cell-free protein synthesis (CFPS) has been employed for synthesis of a potpourri of complex difficult-to-express membrane proteins including voltage-gated ion channels [5]. The eukaryotic CHO-CFPS system is ideally suitable for synthesis of membrane proteins due to the availability of microsomes in the lysate

Abbreviations: nMV, native membrane vesicles; CHO, chinese hamster ovary; CFPS, cell-free protein synthesis; Nav_v, voltage-gated sodium channel; TEVC, two-electrode voltage clamp.

* Corresponding author.

E-mail address: srujan.dondapati@izi-bb.fraunhofer.de (S.K. Dondapati).

<https://doi.org/10.1016/j.bbamem.2023.184144>

Received 21 December 2022; Received in revised form 10 February 2023; Accepted 28 February 2023

Available online 6 March 2023

0005-2736/© 2023 The Authors. Published by Elsevier B.V. This is an open access article under the CC BY-NC-ND license (<http://creativecommons.org/licenses/by-nc-nd/4.0/>).

allowing incorporation into the membrane. These lysates have successfully been utilized for synthesis of large membrane proteins and direct on-chip electrophysiological analysis [6]. Extending the capabilities of the CHO-CFPS, here we attempt to use an approach for generation of a high-molecular weight 24 transmembrane sodium channel.

We prepared and tested cell-free (CF) and cell-based (CB) nMVs harbouring the 220 kDa human cardiac voltage-gated sodium channel (hNav_v1.5) as a proof-of-concept of our approach. Nav_v1.5 is one of the nine voltage-gated sodium channel- α subunits (VGSC- α family) and the key regulators of cardiac rhythm. The rapid inward sodium current (I_{Na}) conducted via the cardiac voltage-gated sodium channel Nav_v1.5 (encoded by SCN5A) is crucial for initiating excitation-contraction coupling in the cardiomyocytes. Last decades of extensive studies of this channel have revealed 400 rare and common genetic variants in SCN5A concomitant to dysfunctions ensuing in life-threatening arrhythmias and structural heart disease [7]. About 1 % of the world's population suffers sudden arrhythmic deaths due to the dysfunction of hNav_v1.5 [8]. Several non-cardiac diseases, including ataxia, epilepsy, pain, bowel syndrome, myotonic dystrophy, and recently cancer relate to a dysfunctional hNav_v1.5 [9]. While the hNav_v1.5 continues to intrigue researchers, we hope to foster rapid high-throughput in-vitro analysis of crucial pharmaceutical proteins such as the hNav_v1.5 with our approach.

Micro-transplantation in *Xenopus* oocytes has evolved as an effective technique for direct in-vitro analysis of membrane preparations. It offers a powerful method for studying neurotransmitter receptors and voltage-operated channels derived from cultured cells or directly from live or post-mortem tissue [10]. These studies have demonstrated that membrane-incorporated receptors and channels injected into *Xenopus* oocytes retain their native electrophysiological properties like sensitivity to blockers. Perhaps, the noteworthy feat of this technique was the micro-transplantation of cell membranes from the brain autopsy of an Alzheimer's patient facilitating direct post-mortem functional characteristics of native membrane protein repertoire [11]. Owing to these advances, *Xenopus* oocytes have yet again gained an interest in their use in the discovery of neurological disorders [12].

Utilizing the vast knowledge from the CFPS, planar lipid bilayers, and micro-transplantation methods, we discuss a multifaceted approach for preparation and electrophysiological characterization using native membranes from cell-free and cell-based methods.

2. Materials and methods

2.1. Cell-free enrichment and detection of de-novo synthesized hNav_v1.5 in native microsomal membranes (CF-nMVs)

In a cell-free approach, we attempted to enrich the microsomal vesicles natively present in CHO-cell free lysate. We performed *de-novo* protein syntheses in coupled transcription/translation reactions in final volume of 25–80 μ l containing 40 % (v/v) translationally active CHO lysate supplemented with HEPES-KOH (pH 7.6, 30 mM, Carl Roth GmbH), Mg(OAc)₂ (3.9 mM, Merck), KOAc (180 mM, Merck), amino acids (complete 100 μ M, Merck), spermidin (0.25 mM, Roche), and energy regenerating components including creatine phosphokinase (0.1 mg/ml, Roche), creatine phosphate (20 mM, Roche), ATP (1.75 mM, Roche) and GTP (0.3 mM, Roche). To allow for DNA transcription during cell-free protein synthesis, 1 U/ μ l T7 RNA polymerase, 0.3 mM of UTP (Roche) and CTP (Roche), and 0.1 mM of the cap analogue m7G (ppp)G (Prof. Edward Darzynkiewicz, Warsaw University, Poland) were added to the reaction. Additionally, PolyG primer (20 μ M, IBA) was added to the reaction. To monitor the protein quantity and quality, cell-free protein synthesis reactions were supplemented with radioactive ¹⁴C-leucine (30 μ M, specific radioactivity 46.15 dpm/pmol, Perkin Elmer). Batch synthesis reactions were incubated at 27 °C for 3 h at 600 rpm (Thermomixer comfort, Eppendorf).

Post a 3 h long reaction, total translation mixture (TM) was fractionated by centrifugation at 16,000 \times g for 10 min into soluble

supernatant (S) and the pelleted microsomal (M) fractions. We monitored ¹⁴C-leucine incorporation in the *de-novo* synthesized hNav_v1.5 protein to determine the production yields. We performed TCA precipitation of the reaction fractions and radioactive scintillation counting for the determination. A pre-cast gradient 4–16 % SDS-PAGE gel (ThermoFisher Scientific) was used to visualize the protein present in the different fractions of the reaction. An auto-radiographic analysis of the synthesized protein was performed under a phosphorimager (Amersham RGB Imager, GE Healthcare) which enabled visualization of the radioactive protein on the SDS-PAGE gel.

2.2. Cultivation of overexpressing cells

CHO-Tet-hNav_v1.5 cells (B'SYS, Switzerland) were cultivated at 37 °C under 5 % CO₂ with Ham's F12 (10 % Fetal calf serum, 2 mM alanylglutamine, Hygromycin, Blastidicin) until 40 % confluency was achieved. Medium was renewed and 1 μ g/ml tetracycline was added for induction. After an incubation period of 24–48 h with roughly 80 %–90 % confluency in the culture, cells were ready for harvest or planar patch-clamp measurements. Control cells (CHO-K1) were treated alike sans the application of antibiotic pressure. We used a tetracycline-inducible Chinese hamster ovary (CHO) cell line over-expressing human Nav_v1.5 receptor (CHO-Tet-hNav_v1.5-GFP) for electrophysiological recordings and membrane isolation. Before harvesting cells for preparation of CB-nMVs, we checked the induced cells for expression of hNav_v1.5 by directly visualizing the fused GFP signal under a fluorescence microscope.

2.3. Patch-clamp recordings

Whole-cell current recordings were performed from harvested CHO-Tet-hNav_v1.5-GFP 24 h after tetracycline induction. Cells were detached using Accutase treatment for 15–20 min at 37 °C. Patch-clamp experiments were performed with an automated patch-clamp system, the Porta-Patch (Nanion Technologies), using borosilicate glass chips with a resistance of 3–5 M Ω . Experiments were performed in internal solution: Nanion internal solution CsF110 (10 mM CsCl, 10 mM NaCl, 110 mM Cs-Fluoride, 10 mM EGTA, 10 mM HEPES/CsOH, pH 7.2, Osmolarity 285 mOsmol) and external solution (140 mM NaCl, 4 mM KCl, 1 mM MgCl₂, 2 mM CaCl₂, 5 mM D-Glucose monohydrate, 10 mM HEPES/NaOH, pH 7.4, Osmolarity 298 mOsmol). The collected data was filtered at 10 kHz (Bessel filter, HEKA amplifier) digitized at a sampling rate of 50 kHz and analysed with Clampfit (Axon instruments) and Origin labs.

2.4. Preparation of cellular membrane vesicles (CB-nMVs)

Membranes were prepared as described by Bazonne et al., 2021. Briefly, ~1 g of the tetracycline induced CHO-K1-hNav_v1.5-GFP cells was collected and disrupted by nitrogen cavitation using the Parr bomb apparatus (Parr Instruments Company, USA). For control, CHO-K1 cells were processed. Cell debris was removed from the sample by centrifugation (6000g, 4 °C, 10 min), and the plasma membrane was isolated by ultracentrifugation (100,000g, 4 °C, 30 min). Plasma membrane vesicles were purified by ultracentrifugation (100,000g, 4 °C, 3 h) in a sucrose gradient (9 ml 45 %, 9 ml 31 %, 6 ml 9 %). The collected interface was concentrated by ultracentrifugation (100,000 g, 4 °C, 30 min), aliquoted, and stored at –80 °C till further use. Using dynamic light scattering (DLS) the size of the CB-nMVs was determined for both the collected fractions. Fluorescence retention was measured in the fractions under a fluorimager (Amersham RGB Imager, GE Healthcare) using a Cy2 laser and confocal microscopy of the sample visualized as a droplet.

2.5. Dot-blot analysis

Blotting was performed using a Bio-Dot (Bio-Rad, USA) micro-filtration apparatus. The anti-hNav_v1.5 antibody (Alomone labs, Israel)

used was raised in a rabbit host and specifically bound the epitope in the cytosolic loop of the hNav_v1.5 protein. We used a secondary horseradish peroxidase (HRP) conjugated anti-rabbit antibody for further detection using an enhanced luminol-based chemiluminescent substrate for the detection of the HRP. To further verify that the protein harboured in our CF- and CB-nMVs was indeed hNav_v1.5, we carried out dot-blot immunoassay with a hNav_v1.5 specific antibody that binds an epitope in the cytosolic loop of the plasma membrane localized protein.

2.6. Micro-transplantation of membrane vesicles into *Xenopus* oocytes

Pre-isolated ready to inject *Xenopus laevis* oocytes were purchased from Ecocyte, Germany. Oocytes were injected with 80 nl plasma membrane vesicles or cell-free enriched microsomes using Roboinject (Molecular Devices GmbH, Germany). Injection needles were filled with RNase free mineral oil before aspiration and injection. The injected oocytes were maintained in modified Barth's solution at 16 °C until electrophysiological recordings were performed. Control oocytes were either un-injected or injected with 80 nl of water.

2.7. Two-electrode voltage clamp recordings from microinjected oocytes

To observe functional hNav_v1.5 responses from the CB-nMVs micro-transplanted in *Xenopus* oocytes, we used the automated two-microelectrode voltage-clamp setup, Robocyte2. 20 h post injection, membrane currents were recorded from voltage-clamped oocytes. Pulled glass microelectrode heads were filled with 3 M KCl and exhibited a resistance of 200 to 1000 MΩ. The oocyte was placed in a recording chamber with continuous perfusion of the MBS (NaCl = 88 mM, KCl = 1 mM, CaCl₂ = 0.4 mM, Ca(NO₃)₂ = 0.33 mM, MgSO₄ = 0.8 mM, TRIS-HCl = 5 mM, NaHCO₃ = 2.4 mM, adjusted to pH 7.4) through a perfusion system at room temperature (20–22 °C). To obtain current response curves, depolarizing pulses were applied in 10 mV step from –100 to +100 mV from a –120 mV deactivation prestep while holding the oocyte membrane potential at –60 mV. Lidocaine solutions of different concentrations were prepared in MBS and then directly applied in the oocyte-containing chamber for 10–20 s using an automated perfusion system. Data were acquired with a pCLAMP system (Digidata 1440 and pCLAMP 10.0 software from Axon Instruments). Data analysis was carried out using Origin labs and GraphPad Prism.

2.8. Single-channel analysis on planar lipid bilayers

Lipid bilayers were formed on a 16 electrode MECA glass chip (Ionera) using the lipid 1,2-diphytanoyl-sn-glycero-3-phosphocholine (DPhPC) at a concentration of 10 mg/ml dissolved in Octane (Sigma Aldrich). The recording solution comprised of 150 mM KCl (Sigma Aldrich (Fluka)) in PBS buffered at pH 7.4. 1 μl of the nMV fraction was added to the 180 μl electrolyte in the measurement chamber for recordings. Lidocaine applications were performed by direct application of the compound into the bath. A multi-channel amplifier (Elements SRL, Italy) was used to acquire multiplexer electronics port of the Orbit16 system. Recordings were done at a sampling rate of 5 kHz with a 500 kHz visual filter. Data were analysed with Clampfit (Molecular Devices, Sunnyvale, CA, USA).

3. Results and discussion

3.1. Cell-free native membranes harbour the hNav_v1.5 protein

Cell-free synthesis of functional membrane proteins remains a challenge. Especially pertaining to large channels like the 24-transmembrane hNav_v1.5 which is classified under the 'difficult-to-express' proteins due to its size and complexity. Due to its open nature, CFPS system allows for optimization of reaction conditions. However, finding the right combination of components is crucial to a successful synthesis.

A big advantage of using the eukaryotic CHO-CFPS system is the availability of microsomes allowing integration of synthesized protein into their native membrane architecture. Utilizing the knowledge and advance in the CHO-CFPS system, we optimized the reaction conditions to enable synthesis of functional hNav_v1.5.

3.1.1. Radiolabelling and autoradiogram analysis

Scintillation records from the incorporated ¹⁴C-leucine in the *de-novo* synthesized hNav_v1.5 protein yielded on an average about 11 μg/ml of total protein as measured in the translational mixture. Post fractionation we observed ~3 μg/ml retained in the microsomal CF-nMVs (Fig. 1a, middle panel). An autoradiogram band observed on a 4–16 % gradient SDS PAGE gel at ~220 kDa corresponded to the size of our cell-free produced hNav_v1.5 (Fig. 1a bottom panel).

3.1.2. Immunodetection of *de-novo* enriched protein in CF-nMVs

Dot-blot further detected the cell-free synthesized hNav_v1.5 in our enriched microsomal nMV (M) as well as in the soluble (S) fraction of the translational mix (TM) (Fig. 1a, bottom panel, right). In the M fraction, the epitope was inaccessible for the antibody and only 1 % Triton X treated nMVs showed a distinct signal. Untreated sample showed a faint signal localized to the periphery of the blot. This may attribute to microsomal aggregates that protect the binding site, or from remnants of the non-membrane bound protein.

Our findings thus far supported the production and successful integration of the *de-novo* synthesized protein into the microsomal membrane and an analysis of its functionality using planar lipid bilayer electrophysiology would further validate our claims. However, to assure that the activity observed on bilayers was indeed from functional CF-nMVs and to exclude any endogenous activity, we performed functional measurements with no-template control reactions (NTC) which served as the negative controls for the CF-nMVs. For ideal comparison, we analysed the functionality of the CB-nMVs under similar conditions on a planar lipid bilayers to the CF-nMVs.

3.2. Cell-based native membranes

3.2.1. Cells expressing hNav_v1.5 under planar patch-clamp conditions

To establish functional expression of the hNav_v1.5 channels in the cells, we observed the expressed GFP signal by direct visualization of the cells under a fluorescence microscope (Supplementary S1a). We briefly tested a few cells under patch-clamp conditions for the voltage-gating characteristics. Under planar patch-clamp conditions, characteristic whole-cell inward sodium currents emanated upon subsequent depolarization of the cell from a hyperpolarized state at –120 mV (Fig. 1b) confirming the expression of functional hNav_v1.5 channels. The currents showed a voltage-sensitive response with the channel peak current amplitudes between –40 mV and –20 mV. Further, depolarization reduced the current amplitudes as the channels inactivated at higher potentials and returned with a complete inactivation at voltages beyond 20 mV.

3.2.2. Size determination of nMVs

The size of the CB-nMVs derived from nitrogen cavitation and sucrose gradient centrifugation was determined by using dynamic light scattering (DLS) for both the collected fractions from the overexpressing cells and the control CHO-K1 cells. All collected samples were rich in nMVs ranging from 230 to 390 nm with subtle difference between each fraction, which may be due to factors such as the size of the expressing cells, and their response to nitrogen cavitation (Fig. 2a). Peak distributions also varied between each sample with fractions from the control larger than the hNav_v1.5 enriched samples. Mean PDI values were 0.246 and 0.377 for 9/31 fractions and 0.406 and 0.471 for the 31/45 fractions of hNav_v1.5 enriched and control samples respectively. The 31/45 fractions showed higher polydispersity for both the control and Nav_v1.5 enriched samples which attributes to presence of a diverse population of

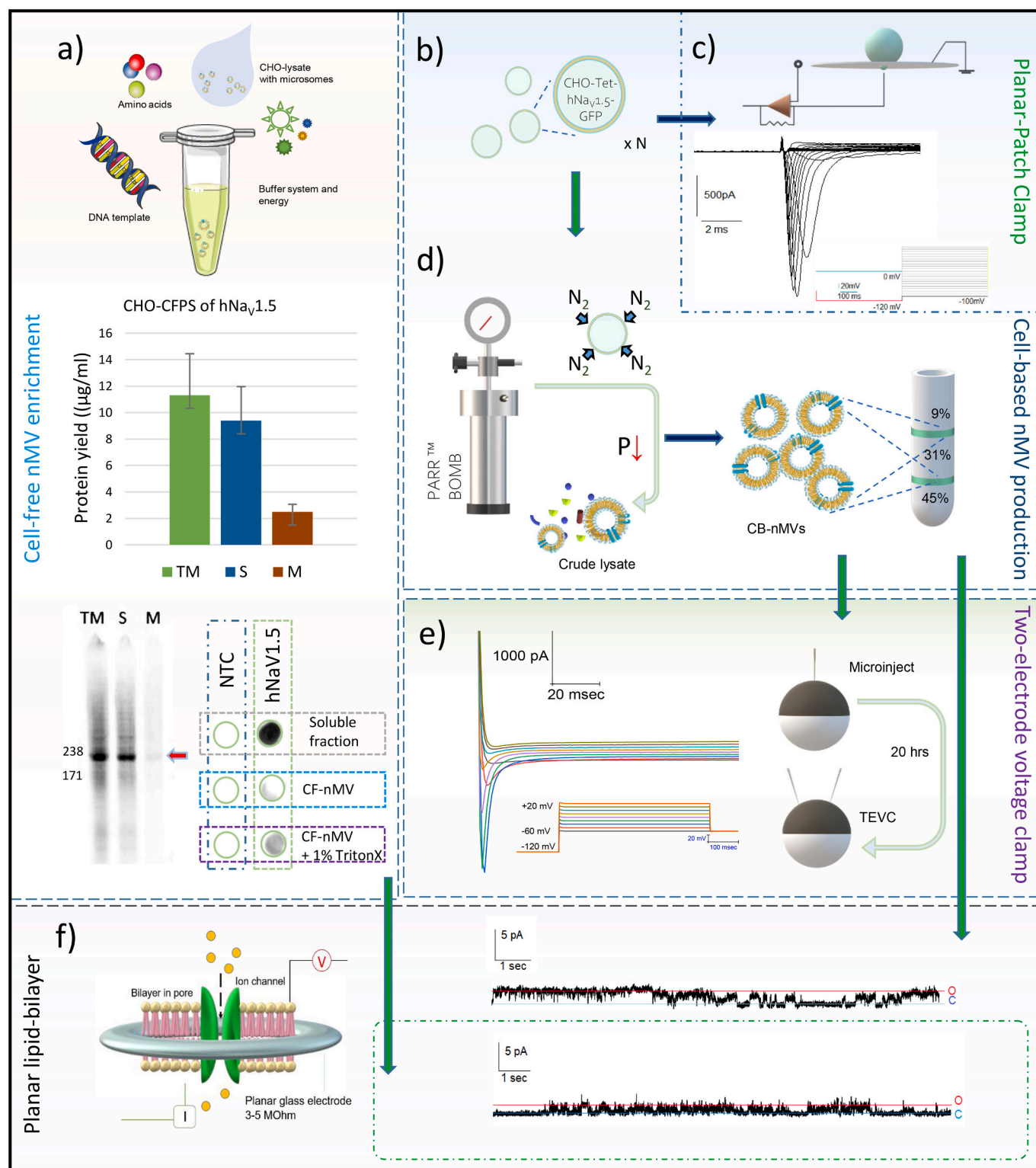


Fig. 1. Graphical depiction of the workflow. a) $hNaV1.5$ was synthesized in a CHO-cell-free protein synthesis platform and enriched microsomal cell-free native membrane vesicles (CF-nMVs) were derived by centrifugation post a 3 h reaction. ^{14}C labelled $hNaV1.5$ was quantified in radioactive leucine supplemented reactions via scintillation counting ($n = 6$; duplicates from 3 reactions). Protein bands visualized via an autoradiogram post fractionation (TM-Translational mix, S-Soluble fraction, M-Microsomal fraction; NTC-No template control) revealed a successful synthesis. The protein was further detected via a dot-blot assay using $hNaV1.5$ specific antibody. b) Wild-type CHO cells and those expressing $hNaV1.5$ were cultured and harvested following an Accutase treatment. c) Cells expressing the $hNaV1.5$ were tested by planar patch-clamp electrophysiology before preparation of the vesicles. Activation currents and voltage protocol used are shown. d) About 1 g of cells were collected and disrupted via nitrogen cavitation in a Parr bomb apparatus and fractionated in a 9–31–45 % sucrose gradient by ultracentrifugation to obtain cell based-native membrane vesicles (CB-nMVs). nMVs from a) and d) were e) Micro-transplanted into *Xenopus* oocytes and only CB-nMVs exhibited currents typical of $hNaV1.5$ after a 24 h incubation(inset), and f) tested on a planar DPhPC bilayer for single-channel properties (conductance level: O-Open, C-Closed). Representative single-channel traces are shown for the cell-based and cell-free nMVs (inset).

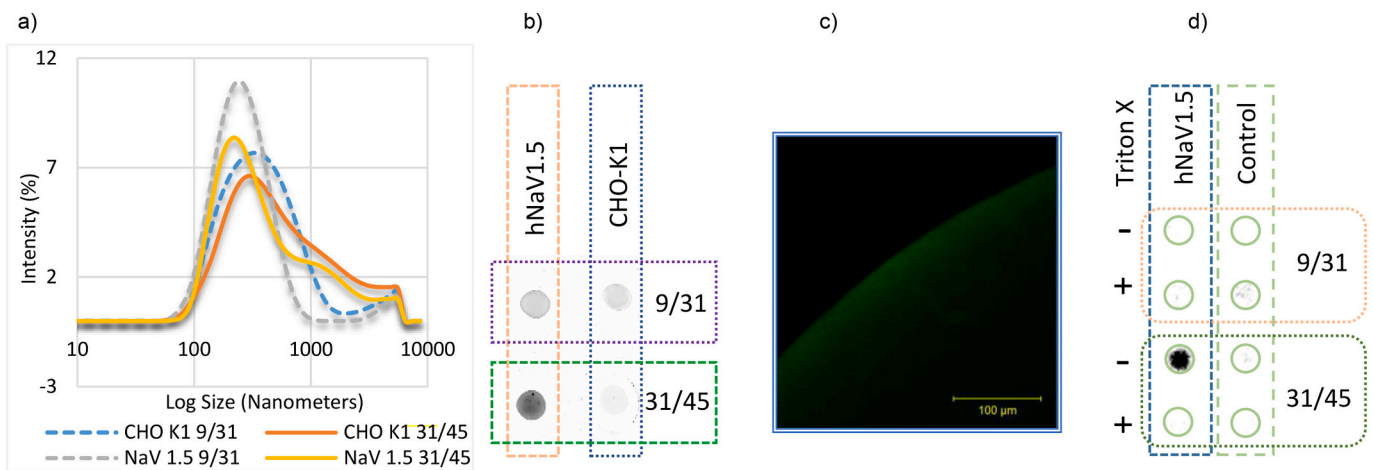


Fig. 2. a) Size of the plasma membrane vesicles as determined by dynamic light scattering. A high polydispersity can be observed in the crude membrane preparations. b) Fluorescence from CB-nMV sample fractions under a fluoroimager visualized using a Cy2 laser c) Fluorescence observed from expressed GFP in the 31/45 hNav_v1.5-GFP CB-nMV fraction as a droplet under a confocal microscope (scale: 100 μ m) d) Dot-blot detected hNav_v1.5 specific antibody signal in the 31/45 fraction of the CB-nMV sample, no distinct signal was observed from the control CHO-K1 nMVs.

membranes in the fraction.

Crude membrane extracts are hence composed of various membrane vesicle sizes which may be directly affected by the size of the original cells, conditions during cavitation and preparation of the lysates. Further fractionation may help increase homogeneity of the population in the samples. However, in order to minimize experimental steps and time from preparation to analysis, this was not carried out.

3.2.3. Fluorescence retention in CB-nMVs

We further tested the CB-nMV samples for retention of their GFP signals. We first performed a quick analysis of the CB-nMV fractions under a fluoroimager (Fig. 2b). Fluorescence observed in the 31/45 fraction of the hNav_v1.5 nMVs was significantly higher than the 9/31 fraction which showed only a faint signal. Control CB-nMVs showed no fluorescence. To closely verify the presence of hNav_v1.5-GFP we then checked all the fractions of nMVs as a droplet under a fluorescence confocal microscope. High fluorescence intensities recorded from the 31/45 fraction were consistent with the fluoroimager observations (Fig. 2c).

3.2.4. Immunodetection of hNav_v1.5 enriched CB-nMVs

A dot-blot performed under similar conditions as the CF-nMVs verified the presence of detectable hNav_v1.5 in the prepared CB-nMVs (Fig. 2d). A strong signal was detected in the 31/45 fraction of the collected nMVs elaborating the high protein content in the fraction. Samples treated with 1 % Triton X appeared to disrupt the detection signal that may be attributed to the action of the detergent on the nMVs and a possible degradation of the binding site. We used the 31/45 CB-nMV fraction for further analysis by planar lipid bilayer electrophysiology due to its enrichment with the protein of interest.

We observed a difference in the action of 1 % Triton X on the cell-based and cell-free nMVs where the detergent disrupted the signal in case of cell-based nMVs while improving it for cell-free nMVs. We performed DLS measurements to determine how the different nMVs reacted to the treatment (Supplementary S2). Triton X appeared to disrupt the cell based vesicles reducing them to small vesicles (<80 nm). For microsomal vesicles the same treatment appeared to have a comparatively smaller effect reducing them to vesicles in the range of 100–120 nm. This is coherent to our hypothesis that the microsomes are incompletely solubilized and may be permeabilized to a retained functional epitope for detection using the antibody. In the study we excluded detailed characterization of antibody-epitope interaction, which might be affected by differences in protein-folding in the two expression

environments.

3.3. Lidocaine sensitivity in cells and nMVs micro-transplanted into *Xenopus* oocytes

The hNav_v1.5 enriched cells retained sensitivity to Lidocaine and responded with a decrease in elicited peak currents upon application of the compound (Fig. 3a). At 20 μ M the currents were reduced to more than half maximal amplitudes. Only a few cells were tested to ensure the cell-line expressed the protein of interest and dose-response curves were hence not derived.

We tested the retention of properties from both the nMVs enriched with hNav_v1.5 protein by micro-transplanting them into *Xenopus* oocytes. For CB-nMVs, two-electrode voltage clamp recordings performed after 20 h of the injections demonstrated whole-cell inward sodium currents characteristic of the expressed protein from both the injected CB-nMV fractions (Figs. 1e, 3b). Oocytes injected with CF-nMVs did not elicit a sodium-specific response. Dose-dependent responses derived from the oocytes at different activation potentials demonstrate exemplary characteristics of blockage of hNav_v1.5 channels by Lidocaine (Fig. 3c). Average value of IC_{50} for Lidocaine inhibitory action on *Xenopus* oocytes ($n = 9$) expressing micro-transplanted CB-nMVs were 1882 μ M and 1332 μ M corresponding to an activation of the hNav_v1.5 at -40 mV and -20 mV respectively. The analysis of CB-nMVs using the mentioned methods established that they were indeed enriched in the hNav_v1.5. Micro-transplantation into *Xenopus* oocytes provided strong proof of their functionality and retention of the Lidocaine sensitivity.

3.4. CF- and CB-nMVs elicit single-channel sodium currents on planar lipid bilayers

After establishing that CB-nMVs harboured functional hNav_v1.5 we directly compared their responses to the CF-nMVs on planar lipid-bilayers. Prior to application of the sample, all empty bilayers were tested by stepping the voltage between -100 mV and $+100$ mV. Any bilayers that responded to the voltage change were shut down to reduce any artefacts from voltage triggered disruptions. All active channels were visually inspected and only channels with cleaner sustained activity were further analysed. Channels with disruptive bilayers, sporadic activity or basal level conductance fluctuations were omitted. On DPhPC lipid bilayers, both the nMVs showed single-channel and ensemble sodium currents under a 150 mM NaCl, pH 7.4 buffer system (Fig. 4a, b). We visually inspected all recorded activity from 183 CB-nMVs, 212 CB-

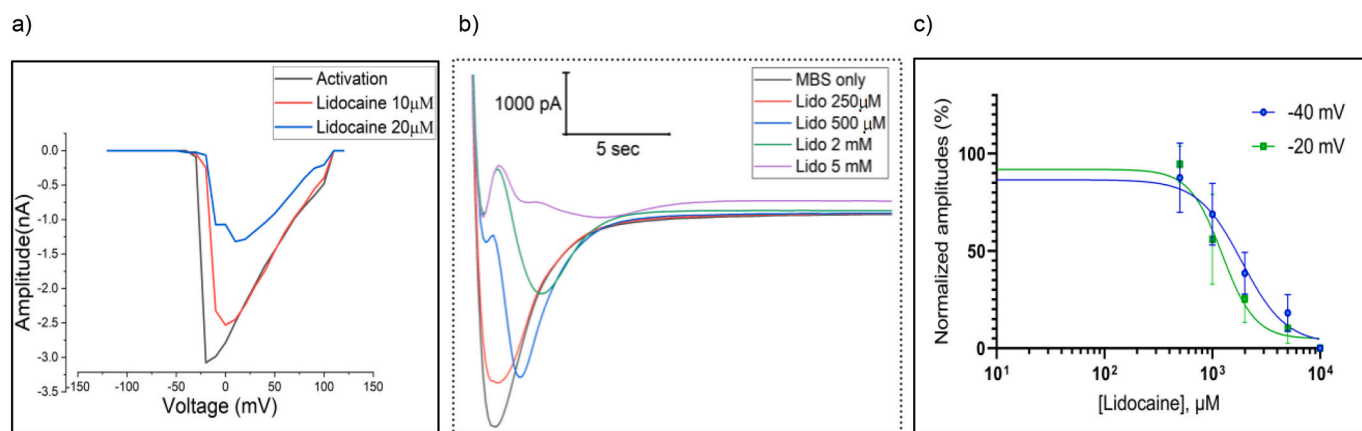


Fig. 3. a) Activation characteristics of expressed hNav_v1.5 in CHO cells under patch-clamp conditions and blockade upon application of Lidocaine. b) Dose-dependent blockage of peak currents at -40 mV and c) Dose-response of *Xenopus* oocytes ($n = 9$) micro-transplanted with CB-nMVs in response to a voltage pulse of -40 mV or -20 mV from a resting voltage of -120 mV (Calculated average IC_{50} 1882 μ M and 1332 μ M respectively).

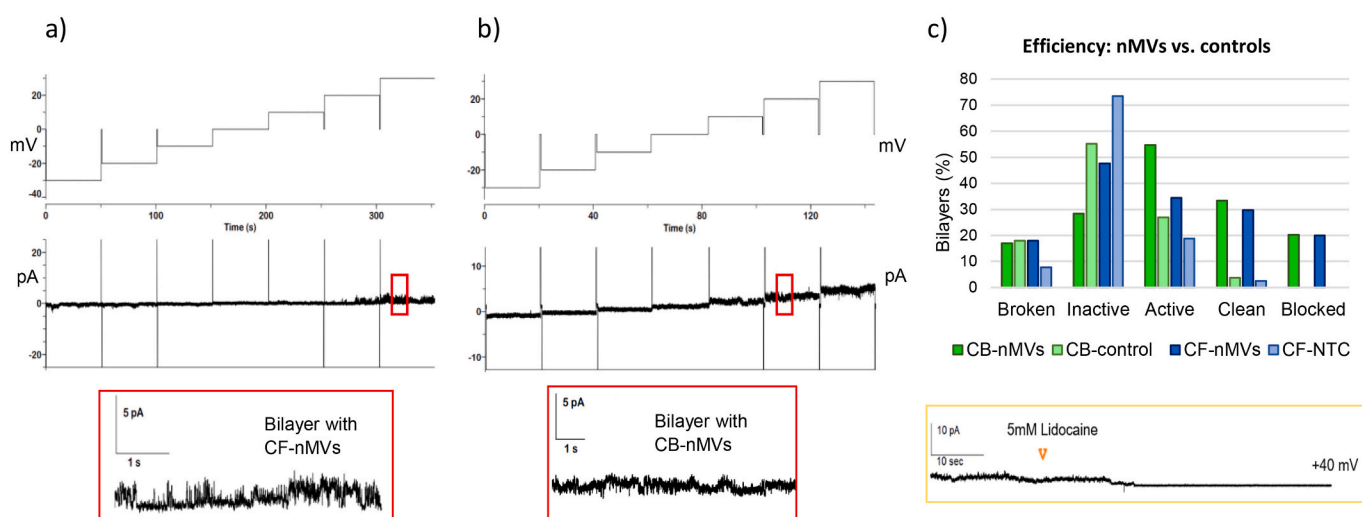


Fig. 4. Single channel currents observed from a DPhPC planar bilayer containing a) CF-nMVs and b) CB-nMVs in response to voltage pulses spanning -30 to $+30$ mV in 10 mV step changes; inset: respective zoomed portions of the current trace marked in red. c) Statistical representation of activity of nMVs on planar lipid-bilayers normalized to total number of bilayers tested (CB-nMVs: 183, CB-control-212, CF-nMVs-131, CF-NTC-117; blocking concentration of 5 mM Lidocaine); inset: exemplary blockade upon addition of 5 mM Lidocaine to an active bilayer containing enriched nMVs.

control, 131 CF-nMVs, 117 CF-NTC bilayers.

For both the nMV preparations, about 30 % of the recorded bilayers exhibited single-channel-like or ensemble currents, with ten-fold higher probability compared to the respective controls (Fig. 4c; control CF-nMVs: no template control, control CB-nMVs: WT CHO-K1 nMVs). From all lipid bilayers recorded, 20 % of the channels responded with complete blockade upon application of 5 mM Lidocaine (Fig. 4c).

CF-nMVs showed a higher sensitivity to lidocaine where a complete block at 5 mM, with most blocked at 2 mM compared with CB-nMVs (about 60 % of active channels blocked at 5 mM) which may be attributed to the difference in the membrane thickness and permeation of Lidocaine across the two types of nMVs. In most observed cases, lidocaine sensitive currents had a uni-directional rectification that was completely lost with 5 mM Lidocaine application (Supplementary S3). In some instances, bidirectional rectifications were observed which might pertain to leaky bilayers that are susceptible to disruption at higher voltages and amenable to non-linear voltage perturbations contributing increased leaks with increasing voltage difference across the membrane [13]. We omitted extensive quantitative statistics of dwell-time, event rate analysis as the currents emanating from the nMVs had varied responses [14], and during recordings, multi-channel insertions were

regular occurrences. A few exemplary traces depicting single-channel activity and corresponding amplitude histograms are represented (Supplementary S4–7). The hNav_v1.5 channels are specifically complicated when comparing their single-channel properties and are known to assemble as dimers [15]. Beyond this hurdle, lidocaine interaction with the lipid bilayer is reported to increase electrostatic potential of the bilayer [16]. Upon lidocaine application, we observed increased current-leaks before the blocking concentration was achieved (Supplementary S8) which reaffirms a non-stationary interaction of the compound with the bilayers.

3.5. Conclusions and perspectives on using native membrane vesicles derived from cellular and cell-free systems

CB-nMVs allow bi-faceted analysis of electrogenic membrane proteins: single-channel analysis on the artificial lipid bilayer platform and whole-cell analysis of micro-transplanted CB-nMVs in *Xenopus* oocytes. Our approach assures that the nMVs generated by the method retain functionality before testing on the contrived planar lipid bilayer platforms. CF-nMVs demonstrate a rapid enrichment of target protein within 3 h, which is unachievable with cellular systems. Unlike liposomes or

giant unilamellar vesicles (GUVs), nMV requires no lipid reconstitution during preparation. Thus, the native membrane environment in which the protein resides remains conserved. Most importantly, on an on-chip lipid-bilayer platform, nMVs can be readily thawed and directly analysed. The CB-nMVs remains functionally stable when frozen for long durations and usable on demand. The cell free nMVs offer the advantage of rapid production which fosters a time efficient analysis on lipid-bilayers. While conventional mRNA-based expression in *Xenopus* oocytes takes 48 h, micro-transplantation of CB-nMVs enables the study of native channel properties within 24 h. Micro-transplantation of the sample thus drastically reduces the time to whole-cell analysis. Apart from the time-effective and storage advantages of native membranes, it is known that membrane proteins especially voltage gated ion channels are very sensitive to lipid composition and charge and measuring their activity in the native membranes will offer an ideal environment for studying the membrane protein behaviour. In case of the CF-nMVs, the scarcity of functional yields of protein for the assay may contribute to the null signals. It has been reported that microsomal membranes tend to reorganise into endoplasmic reticular structures when micro-transplanted into the *Xenopus* oocyte [17]. Microsomes may transit the cellular machinery differently than plasma membrane vesicles owing to dissimilarity in the size, lipid composition, presence of micro-tubular structures and accessory proteins. This may contribute to the differences in the micro-transplantation efficiency of injected nMVs. We aim at exploring this in future studies to substantiate whether microsomal derived membranes can be translocated to transplant onto *Xenopus* oocytes plasma membranes and improve the system for testing functionality of cell-free produced proteins.

CRedit authorship contribution statement

Yogesh Pandey: Conceptualization, Methodology, Formal analysis, Investigation, Visualization, Writing – original draft, Writing – review & editing. **Srujan Dondapati:** Conceptualization, Supervision, Project administration, Writing – review & editing. **Stefan Kubick:** Resources, Funding acquisition.

Declaration of competing interest

The authors declare that they have no known competing financial interests or personal relationships that could have appeared to influence the work reported in this paper.

Acknowledgements

We would like to thank Wenzel, D for providing the lysates used and Andersson, A for their help at the cell-culture facility. This research was funded by the Ministry of Science, Research and Culture (MWFK, Brandenburg, Germany), project PZ-Syn (project number F241-03-FhG/005/001), and the Federal Ministry of Education and Research (BMBF, Germany, Nos. 13GW0408C).

Appendix A. Supplementary data

Supplementary data to this article can be found online at <https://doi.org/10.1016/j.bbmem.2023.184144>.

[org/10.1016/j.bbmem.2023.184144](https://doi.org/10.1016/j.bbmem.2023.184144).

References

- [1] a) Bertil Hille, Ion-Channels-of-Excitable-Membranes, 2001; N. Gamper, J.D. Stockand, M.S. Shapiro, Journal of pharmacological and toxicological methods 51 (2005) 177.
- [2] a) A. Williams, N.L. Thomas, in: G. Roberts, A. Watts (Eds.), Encyclopedia of Biophysics, Springer Berlin Heidelberg, Berlin, Heidelberg, 2019, pp. 1–11; b) R.P. Hartshorne, B.U. Keller, J.A. Talvenheimo, W.A. Catterall, M. Montal, Proceedings of the National Academy of Sciences of the United States of America (1985) 240; c) M. Garten, L.D. Mosgaard, T. Bornschlög, S. Dieudonné, P. Bassereau, G.E. S. Toombes, Proceedings of the National Academy of Sciences of the United States of America 114 (2017) 328; d) M. Komiya, T. Ma, D. Tadaki, A. Hirano-Iwata, Bunseki kagaku 67 (2018) 749.
- [3] K. Kamiya, T. Osaki, K. Nakao, R. Kawano, S. Fujii, N. Misawa, M. Hayakawa, S. Takeuchi, Sci. Rep. 8 (2018) 17498.
- [4] a) A. Bazzone, A. Körner, M. Meincke, M. Bhatt, S. Dondapati, M. Barthmes, S. Kubick, N. Fertig, Biosensors & bioelectronics 197 (2022), 113763; b) J. Wang, R. Terrasse, J.A. Bafna, L. Benier, M. Winterhalter, Angewandte Chemie (International ed. in English) 59 (2020), 8517.
- [5] a) N.E. Gregorio, M.Z. Levine, J.P. Oza, Methods and protocols (2019) 2; b) X. Jin, S.H. Hong, Biochem. Eng. J. 138 (2018) 156.
- [6] L. Thoring, S.K. Dondapati, M. Stech, D.A. Wüstenhagen, S. Kubick, Sci. Rep. 7 (2017) 11710.
- [7] a) A.A.M. Wilde, A.J. Moss, E.S. Kaufman, W. Shimizu, D.R. Peterson, J. Benhorin, C. Lopes, J.A. Towbin, C. Spazzolini, L. Crotti, et al., Circulation 134 (2016) 872; b) M. Liu, K.-C. Yang, S.C. Dudley, Curr. Top. Membr. 78 (2016) 513.
- [8] C.R. Bezzina, N. Lahrouchi, S.G. Priori, Circ. Res. 2015 (2015) 116.
- [9] a) P. Gotra, N. Bhardwaj, A. Ludhiadch, G. Singh, A. Munshi, Mol. Neurobiol. 58 (2021) 3874; b) S.P. Fraser, R. Onkal, M. Theys, F. Bosmans, M.B.A. Djamgoz, Br. J. Pharmacol. 179 (2022) 473; c) S.P. Fraser, I. Ozerlat-Gunduz, W.J. Brackenbury, E.M. Fitzgerald, T. M. Campbell, R.C. Coombes, M.B.A. Djamgoz, Philosophical transactions of the Royal Society of London Series B, Biological sciences 369 (2014) 20130105; d) H. Rajaratnam, N.F. Mokhtar, N. Asma-Abdullah, W.E.M. Fuad, Biomolecules (2022) 12; e) B.T. Priest, M.L. Garcia, R.E. Middleton, R.M. Brochu, S. Clark, G. Dai, I.E. Dick, J.P. Felix, C.J. Liu, B.S. Reiseter, et al., Biochemistry 43 (2004) 9866; f) Y.A. Saito, P.R. Strege, D.J. Tester, G.R. Locke, N.J. Talley, C.E. Bernard, J. L. Rae, J.C. Makielski, M.J. Ackerman, G. Farrugia, American journal of physiology Gastrointestinal and liver physiology 296 (2009) G211–G218.
- [10] a) J. Paiement, F.W. Kan, J. Lanoix, M. Blain, The journal of histochemistry and cytochemistry: official journal of the Histochemistry Society 36 (1988) 1263; b) F. Mazzo, R. Zwart, G.M. Serratto, K.M. Gardinier, W. Porter, J. Reel, G. Maraula, E. Sher, Journal of neurochemistry 138 (2016) 384; c) L.A. Maia, I. Velloso, J.G. Abreu, Expert opinion on drug discovery 12 (2017) 1153; d) Eleonora Palma, Flavia Trettel, Sergio Fucile, Massimiliano Renzi, Ricardo Miledi, Fabrizio Eusebi, Proceedings of the National Academy of Sciences of the United States of America 100 (2003) 2896; e) J. Marsal, G. Tigyi, R. Miledi, Proceedings of the National Academy of Sciences of the United States of America (1995) 5224.
- [11] J. Parodi, L. La Ochoa-de Paz, R. Miledi, A. Martínez-Torres, Molecules and cells 34 (2012) 349.
- [12] a) S.L. Zeng, L.C. Sudlow, M.Y. Berezin, Expert Opin. Drug Discovery 15 (2020) 39; b) B. Miller, N. Moreno, B.A. Gutierrez, A. Limon, Membranes (2022) 12.
- [13] Kamran C. Melikov, Vadim A. Frolov, Arseniy Shcherbakov, Andrey V. Samsonov, Yury A. Chizmadzhev, Leonid V. Chernomordik, Biophys. J. 2001 (1829) 80.
- [14] R. Nishiguchi, T. Tanaka, J. Hayashida, T. Nakagita, W. Zhou, H. Takeda, Membranes (2022) 13.
- [15] J. Clatot, M. Hoshi, X. Wan, H. Liu, A. Jain, K. Shinlapawittayatorn, C. Marionneau, E. Ficker, T. Ha, I. Deschênes, Nat. Commun. 8 (2017) 2077.
- [16] C.-J. Högberg, A.P. Lyubartsev, Biophys. J. 94 (2008) 525.
- [17] J. Paiement, J.M. Dominguez, J. McLeese, J. Bernier, L. Roy, M. Bergeron, Am. J. Anat. (1990) 183.